

Aberystwyth University

A microbial ecosystem beneath the West Antarctic ice sheet

Christner, Brent C.; Priscu, John C.; Achberger, Amanda M.; Barbante, Carlo; Carter, Sasha P.; Christianson, Knut; Michaud, Alexander B.; Mikucki, Jill A.; Mitchell, Andy; Skidmore, Mark L.; Vick-Majors, Trista J.; Science Team, The WISSARD

Published in:
Nature

DOI:
[10.1038/nature13667](https://doi.org/10.1038/nature13667)

Publication date:
2014

Citation for published version (APA):

Christner, B. C., Priscu, J. C., Achberger, A. M., Barbante, C., Carter, S. P., Christianson, K., Michaud, A. B., Mikucki, J. A., Mitchell, A., Skidmore, M. L., Vick-Majors, T. J., & Science Team, T. WISSARD. (2014). A microbial ecosystem beneath the West Antarctic ice sheet. *Nature*, 512(7514), 310-313.
<https://doi.org/10.1038/nature13667>

General rights

Copyright and moral rights for the publications made accessible in the Aberystwyth Research Portal (the Institutional Repository) are retained by the authors and/or other copyright owners and it is a condition of accessing publications that users recognise and abide by the legal requirements associated with these rights.

- Users may download and print one copy of any publication from the Aberystwyth Research Portal for the purpose of private study or research.
- You may not further distribute the material or use it for any profit-making activity or commercial gain
- You may freely distribute the URL identifying the publication in the Aberystwyth Research Portal

Take down policy

If you believe that this document breaches copyright please contact us providing details, and we will remove access to the work immediately and investigate your claim.

tel: +44 1970 62 2400
email: is@aber.ac.uk

A microbial ecosystem beneath the West Antarctic Ice Sheet

Brent C. Christner^{1*}, John C. Prisco^{2*}, Amanda M. Achberger¹, Carlo Barbante³, Sasha P. Carter⁴, Knut Christianson^{5,9}, Alexander B. Michaud², Jill A. Mikucki⁶, Andrew C. Mitchell⁷, Mark L. Skidmore⁸, Trista J. Vick-Majors², & the WISSARD Science Team

¹ Department of Biological Sciences, Louisiana State University, Baton Rouge, LA, USA;

² Department of Land Resources and Environmental Science, Montana State University, Bozeman, MT, USA;

³ Institute for the Dynamics of Environmental Processes – CNR, Venice, and Department of Environmental Sciences, University of Venice, Venice, Italy;

⁴ Institute of Geophysics and Planetary Physics, Scripps Institution of Oceanography, University of California San Diego, La Jolla, CA, USA;

⁵ Physics Department, St. Olaf College, Northfield, MN, USA;

⁶ Department of Microbiology, University of Tennessee, Knoxville, TN, USA;

⁷ Department of Geography and Earth Sciences, Aberystwyth University, Aberystwyth, UK;

⁸ Department of Earth Science, Montana State University, Bozeman, MT, USA;

⁹ Present address: Courant Institute of Mathematical Sciences, New York University, New York, NY, USA

* Correspondence should be addressed to B.C.C. (xner@lsu.edu) or J.C.P. (jprisco@montana.edu)

Liquid water has been known to occur beneath the Antarctic Ice Sheet for more than 40 years¹, but only recently have these subglacial aqueous environments been recognized as microbial ecosystems that may influence biogeochemical transformations on a global scale²⁻⁴. Here we present the first geomicrobiological description of water and surficial sediments obtained from direct sampling of a subglacial Antarctic lake. Subglacial Lake Whillans (SLW) lies beneath ~800 m of ice on the lower portion of the Whillans Ice Stream (WIS) in West Antarctica and is part of an extensive and evolving subglacial drainage network⁵. The water column of SLW contained metabolically active microorganisms and was derived primarily from glacial ice melt with solute sources from lithogenic weathering and a minor seawater component. Heterotrophic and autotrophic production data together with small subunit rRNA (SSU rRNA) gene sequencing and biogeochemical data indicate that SLW is a chemosynthetically driven ecosystem inhabited by a diverse assemblage of bacteria and archaea. Our results confirm that aquatic environments beneath the Antarctic Ice Sheet support viable microbial ecosystems, corroborating previous reports suggesting they contain globally relevant pools of carbon and microbes^{2,4} that can mobilize elements from the lithosphere⁶ and influence Southern Ocean geochemical and biological systems⁷.

Almost 400 subglacial lakes have been identified beneath the Antarctic Ice Sheet⁸. Speculation on the presence of functional microbial ecosystems within these lakes followed their discovery¹ and motivated the initial studies of samples originating from Subglacial Lake Vostok (SLV)^{9,10}. However, the body of microbiological data from SLV has been a point of contention, primarily because all studies were based on analyses of frozen (i.e., accreted) lake water samples recovered from a borehole containing a contaminated hydrocarbon drilling fluid³. Our report

documents the first analysis of water and surficial sediments collected directly from a subglacial lake beneath the West Antarctic Ice Sheet (WAIS) using microbiologically clean drilling and sampling techniques¹¹.

The water residence time for SLV exceeds 10,000 years¹², while that for “active” lakes such as SLW is on the order of years to decades^{5,8}. SLW is part of a network of three major reservoirs beneath the lower ice plain of the WIS that regulate water transport to a subglacial estuary at the grounding zone, linking the hydrological system to the sub-ice-ocean cavity beneath the Ross Ice Shelf^{5,13} (Fig. 1). During two separate drainage events in 2006 and 2009, SLW discharged $\sim 0.15 \text{ km}^3$ of water over two six month periods, each time lowering the lake level by $\sim 5 \text{ m}$ ^{5,14}. The drilling location to access SLW was selected using reflection seismology¹³ and ice-penetrating radar¹⁴ data, and corresponded to the region of maximum predicted water column thickness, lowest hydropotential, and largest satellite-measured surface elevation changes (Fig. 1).

A hot water drilling system was used to create a $\sim 0.6 \text{ m}$ diameter borehole through the overlying ice sheet into SLW, allowing for physical measurements and the direct collection of water column and sediment samples. Drilling and lake entry procedures followed recommendations for environmental protection of subglacial aquatic environments¹¹, incorporating rigorous measures to reduce the introduction of foreign microbiota and material into SLW and the interconnected subglacial drainage system. Video inspection of the borehole and temperature measurements revealed that the ice-water interface occurred at 801 ± 1 meters below the surface (mbs) and the lake depth at the borehole site was $\sim 2.2 \text{ m}$ at the time of sampling. Two borehole deployments of a conductivity, temperature, and depth (CTD) sonde together with data from three discrete hydrocasts showed that SLW had an average in situ

temperature of -0.49°C , pH of 8.1, and conductivity of $720\ \mu\text{S cm}^{-1}$; properties that were distinctly different from the borehole water (Table 1).

Water from three discrete hydrocasts in SLW had near identical geochemical compositions based on major ion chemistry (Table 1) and all showed oxygen under-saturation (~16% of air saturated water). Since there is no definitive evidence of lake water freezing to the bottom of the overlying ice sheet as in SLV¹², it is unlikely that lake water constituents in SLW are influenced significantly by freeze concentration. The $\delta^{18}\text{O-H}_2\text{O}$ for SLW (-38.0‰) was similar to glacial ice sampled ~10 m above the ice-water interface from the neighboring Kamb Ice Stream¹⁵ (KIS; -38 to -39‰), indicating that glacial melt was the dominant water source for SLW. A considerable fraction of the major anions and cations originated from mineral weathering, with a minor seawater component based on Cl^- to Br^- ratios (Extended Data Table 1). Crustally-derived non-seawater solutes in SLW showed a dominance of weathering products from silicate minerals ($\text{Na}^+ + \text{K}^+$) over carbonate minerals ($\text{Mg}^{2+} + \text{Ca}^{2+}$), similar to other sub ice-sheet systems in Greenland and Antarctica^{6,7} (Supplemental Discussion). The dominant non-seawater anions (SO_4^{2-} and HCO_3^-) were likely products of sulfide oxidation, carbonation reactions, and carbonate dissolution⁷. Sulfide oxidation and carbonation reactions have been demonstrated to be microbially driven in subglacial systems and linked to enhanced rates of mineral weathering¹⁶. Although clay minerals are a potential source of the relatively high F^- concentrations in SLW (Table 1), subglacial volcanism in the upstream catchment supplying SLW¹⁷ may also contribute.

Ammonium accounted for 73% of the dissolved inorganic nitrogen pool within the water column of SLW (Table 1). Given that mineral sources of ammonium are minor, the majority of the ammonium is likely from microbial mineralization. Soluble reactive phosphorus levels were

70 similar to the total inorganic nitrogen pool (dissolved N:P molar ratio of 1.1), implying a
biologically nitrogen deficient environment, relative to phosphorus. Unfortunately, sample
limitations precluded measurement of dissolved organic N and P concentrations to assess their
nutritional contribution. In addition to its nutritional role, ammonium is also an energy source for
chemolithoautotrophic ammonium oxidizing bacteria and archaea. Evidence for complete
75 nitrification in the aerobic SLW water column was supported by $\Delta^{17}\text{O-NO}_3$ values (-0.1 ‰ to 0.2
‰) that indicated microbial processes rather than atmospheric input was the dominant source for
nitrate in the lake¹⁸. Particulate organic C (PC) to N (PN) molar ratios in the water column
exceeded that of actively growing bacteria by almost 15-fold, suggestive of elevated levels of
nitrogen poor detritus. Dissolved organic carbon (DOC) in the water column averaged 221 ± 55
80 $\mu\text{mol L}^{-1}$, which is ~five times greater than average values for the deep ocean¹⁹ and similar to the
maximum range estimate for SLV^{9,20} (86-160 $\mu\text{mol L}^{-1}$). Acetate and formate concentrations in
the water column averaged 1.3 and 1.2 $\mu\text{mol L}^{-1}$, respectively, indicating that at least a portion of
the DOC pool was labile. The conductivity and microbiological data (Table 1 and Figure 3)
showed that little mixing occurred between the borehole water and lake, supporting that DOC in
85 the water column originated from SLW. The lack of winnowing in sediment cores from SLW, in
concert with the fact that similar DOC concentrations were obtained as the overlying ice moved
~4m during the course of our science operations, provided evidence that water column DOC did
not result from sediment disturbance during drilling operations. The DOC in SLW most likely
originates from upward diffusion of DOC associated with ancient marine sediments⁴ (SLW
90 sediment surface area: depth ratio ~30,000), chemoautotrophic production, or from a
combination of both sources.

The average cell density in the SLW water column was 1.3×10^5 cell mL⁻¹ (Table 1); microscopy revealed the presence of numerous morphotypes, approximately 10% of which were filamentous (Fig. 2). Cellular ATP, a proxy for viable biomass, in SLW was 3.7 pmol ATP L⁻¹ (Table 1). Cell and ATP concentrations were 188- and 93-fold higher, respectively, than those observed in the borehole water before breakthrough to SLW. Carbon biomass estimates for SLW water based on the ATP data (480 ± 100 ng C L⁻¹) were 3 to 50-fold higher than those observed beneath the Ross Ice Shelf at site J9²¹. Analysis of SSU rRNA sequences amplified from the water column samples showed that the community was similar among replicate lake samples, was distinct from the drilling water (Fig. 3a), and contained at least 3,931 operational taxonomic units (OTUs; Extended Data Table 2). An OTU closely related to the nitrite oxidizing betaproteobacterium '*Candidatus Nitrotoga arctica*'²² comprised 13% of the sequence data, and many of the most abundant phylotypes were closely related to chemolithoautotrophic species that use reduced nitrogen, iron, or sulfur compounds as energy sources (Fig. 3b; Supplemental Discussion). Two of the abundant water column OTUs had high identity (>99%) to SSU sequences previously reported from sediments sampled beneath the KIS²³ (Fig. 3b). Preliminary attempts to detect eukaryotic SSU sequences in the SLW water column were unsuccessful.

Average dark ¹⁴C-bicarbonate incorporation in the water column samples (32.9 ng C L⁻¹ d⁻¹; Table 1) exceeded average rates of heterotrophic production based on ³H-thymidine (13.7 ng C L⁻¹ d⁻¹) and ³H-leucine (2.9 ng C L⁻¹ d⁻¹) incorporation by 2- and 11-fold, respectively.

Assuming that the thymidine and leucine values represent net incorporation, and that respiratory losses were 87% of net incorporation (i.e., average for Antarctic McMurdo Dry Valley lakes²⁴), the gross bacterial carbon demand (net productivity + respiration) would be 105 and 23 ng C L⁻¹ d⁻¹, respectively. If dark ¹⁴C-bicarbonate incorporation represents new organic carbon production

115 via chemoautotrophy, the observed rates would meet between 31% and 143% of the heterotrophic carbon demand in the system. It should be noted that the effect of pressure (~ 8 MPa in SLW) was not tested and may influence the absolute rates of metabolism measured.

Pore water conductivity ($860 \mu\text{S cm}^{-1}$) and pH (7.3) in SLW's surficial sediments were within 20% of the lake water values (Table 1). Upward diffusion of ions from sediment pore

120 water is presumably the primary source of the ions in the water column. Average surficial sediment PC and PN concentrations were 384.2 and $21.5 \mu\text{mol g dry wt}^{-1}$, respectively, and represented 0.43% and 0.03% of sediment dry weight. The molar PC:PN ratio in the surficial sediment layer (17.9) was 3.7 times lower than that in water column (Table 1), indicative of nitrogen enriched sedimentary particulate organic matter, with respect to water column

125 suspensoids. Based on rates of thymidine and leucine incorporation, average heterotrophic production in the surficial sediment was 46.6 and $0.9 \text{ ng C d}^{-1} \text{ g dry wt}^{-1}$, respectively.

Approximately 75% of the OTUs from the surficial sediments classified within the Proteobacteria (Fig. 3a). Although many phylotypes in the water column were also abundant in the surficial sediments (Fig. 3b), ~70% of the OTUs were unique to the sediment environment.

130 The nearest neighbors of the most abundant phylotypes in the surface sediments were chemolithoautotrophs or species that use C1 hydrocarbons as carbon and energy sources (Fig. 3b, Supplemental Discussion).

Our data show that SLW supports a metabolically active and phylogenetically diverse ecosystem that functions in the dark at subzero temperatures, confirming more than a decade of
135 circumstantial evidence regarding the presence of life beneath Antarctica's ice sheet^{9,10,21,23}. Rate experiments revealed that chemoautotrophic primary production in SLW is adequate to support heterotrophic metabolism in the subglacial ecosystem. The abundance of taxa related to

nitrifiers^{22,25} in concert with elevated ammonium and $\Delta^{17}\text{O-NO}_3$ values near 0 ‰ in the water column (Table 1) implies that nitrification may be a fundamental chemoautotrophic pathway of new organic carbon production in SLW. Similar conclusions regarding the ecological significance of nitrification have been drawn for the water column beneath the Ross Ice Shelf²⁶ and in McMurdo Sound²⁷. Given the prevalence of subglacial water in Antarctica⁸, our data from SLW lead us to contend that aquatic microbial ecosystems are common features of the subsurface environment that exists beneath the $\sim 10^7 \text{ km}^2$ Antarctic Ice Sheet, which may have significant roles in stimulating Southern Ocean primary productivity⁷.

Accepted 9 July 2014

References

1. Oswald, G. K. A. & Robin, G.De.Q. Lakes beneath the Antarctic Ice Sheet. *Nature* 245,
150 251-254 (1973)
2. Priscu, J. C. et al. Antarctic subglacial water: origin, evolution and ecology. In: Vincent,
W. & Laybourn-Parry, J. (eds), *Polar Lakes and Rivers* (Oxford University, 2008)
3. Christner, B. C., Skidmore, M. L., Priscu, J. C., Tranter, M. & Foreman, C.M. Bacteria in
subglacial environments. In: Margesin, R., Schinner, F., Marx. J.-C. & Gerday, C. (eds)
155 *Psychrophiles: From Biodiversity to Biotechnology* (Springer 2008)
4. Wadham, J. L. et al. Potential methane reservoirs beneath Antarctica. *Nature* 488, 633-
637 (2012)
5. Fricker, H. A., Scambos, T., Bindschadler, R. & Padman, L. An active subglacial water
system in West Antarctica mapped from space. *Science* 315, 1544-1548 (2007)
6. Skidmore, M., Tranter, M., Tulaczyk, S. & Lanoil, B. Hydrochemistry of ice stream beds
160 - evaporitic or microbial effects? *Hydrol. Process.* 24, 517-523 (2010)
7. Wadham, J. L. et al. Biogeochemical weathering under ice: size matters. *Global
Biogeochem. Cycles* 24, GB3025, doi:10.1029/2009GB003688 (2010)
8. Wright, A. & Siegert, M. A fourth inventory of Antarctic subglacial lakes. *Antarct. Sci*
165 24, 659-664 (2012)
9. Priscu, J. C. et al. Geomicrobiology of subglacial ice above Lake Vostok, Antarctica.
Science 286, 2141-2144 (1999)
10. Karl, D. M. et al. Microorganisms in the accreted ice of Lake Vostok, Antarctica. *Science*
286, 2144-2147 (1999)

11. Priscu, J. C. *et al.* A microbiologically clean strategy for access to the Whillans Ice Stream subglacial environment. *Antarct. Sci.* 25, 637-647 (2013)
12. Bell, R. E. *et al.* Origin and fate of Lake Vostok water frozen to the base of the East Antarctic ice sheet. *Nature* 416, 307-310 (2002)
13. Horgan, H. J. *et al.* Estuaries beneath ice sheets. *Geology* 41, 1159-1162 (2013)
14. Christianson, K., Jacobel, R. W., Horgan, H. J., Anandakrishnan, S. & Alley, R. B. Subglacial Lake Whillans—Ice-penetrating radar and GPS observations of a shallow active reservoir beneath a West Antarctic ice stream. *Earth Planet. Sci. Lett.* 331-332, 237-245 (2012)
15. Vogel, S. W. *et al.* Subglacial conditions during and after stoppage of an Antarctic Ice Stream: is reactivation imminent? *Geophys. Res. Lett.* 32, L14502 (2005)
16. Montross, S. N., Skidmore, M., Tranter, M., Kivimäki, A.-L. & Parkes, R. J. A microbial driver of chemical weathering in glaciated systems. *Geology* 41, 215–218 (2013)
17. Blankenship, D. D., Bell, R. E., Hodge, S. M., Brozena, J. M., Behrendt, J. C. & C. A. Finn. Active volcanism beneath the West Antarctic Ice-sheet and implications for Ice-sheet stability. *Nature* 361, 526–529 (1993)
18. Michalski, G., Bhattacharya, S. K. & Girsch, G. NO_x cycle and tropospheric ozone isotope anomaly: an experimental investigation. *Atmos. Chem. Phys. Discuss.* 13, 9443-9483 (2003)
19. Hansell, D. A. & Carlson, C. A. Deep-ocean gradients in the concentration of dissolved organic carbon. *Nature* 395, 263-266 (1998)
20. Christner, B. C. *et al.* Limnological conditions in Subglacial Lake Vostok, Antarctica. *Limnol. Oceanogr.* 51, 2485-2501 (2006)

21. Azam, F. *et al.* Occurrence and metabolic activity of organisms under the Ross Ice Shelf, Antarctica, at Station J9. *Science* 203, 451-453 (1979)
- 195 22. Alawi, M., Lipski, A., Sander, T. Mari-Pfeiffer, E. & Spieck, E. Cultivation of a novel cold-adapted nitrite oxidizing betaproteobacterium from the Siberian Arctic. *ISME J* 7, 256-264 (2007)
23. Lanoil, B. *et al.* Bacteria beneath the West Antarctic Ice Sheet. *Environ. Microbiol.* 11, 609-615 (2009)
- 200 24. Takacs, C, Priscu, J. & McKnight, D. Bacterial dissolved organic carbon demand in McMurdo Dry Valley Lakes, Antarctica. *Limnol. Oceanogr.* 46, 1189–1194 (2001)
25. Walker, C.B. *et al.* *Nitrosopumilus maritimus* genome reveals unique mechanisms for nitrification and autotrophy in globally distributed marine crenarchaea. *Proc. Natl. Acad. Sci. USA* 107, 8818-8823 (2010)
- 205 26. Horrigan, S. G. Primary production under the Ross Ice Shelf, Antarctica. *Limnol Oceanogr* 26, 378-382 (1981)
27. Priscu, J. C., Downes, M. T., Priscu, L. R., Palmisano, A. C. & Sullivan, C. W. Dynamics of ammonium oxidizer activity and nitrous oxide (N₂O) within and beneath Antarctic Sea Ice. *Mar. Ecol. Prog. Ser.* 62, 37-46 (1990)
- 210 28. Fricker, H. A. & Scambos, T. Connected subglacial lake drainage activity on lower Mercer and Whillans Ice Streams, West Antarctica, 2003-2008. *J. Glaciol.* 55, 303-315 (2009)
29. Depoorter, M. A., *et al.* Calving fluxes and basal melt rates of Antarctic ice shelves. *Nature* 502, 89-92 (2013)

- 215 30. Haran, T., Bohlander, J., Scambos, T. & Fahnestock, M. MODIS mosaic of Antarctica
(MOA) image map. Boulder, Colorado USA: National Snow and Ice Data Center,
<http://dx.doi.org/10.7265/N5ZK5DM5> (2005)

Accepted 9 July 2014

220 **Methods**

Site selection and description. SLW was discovered using satellite laser altimetry and initially identified as a region ($59 \pm 12 \text{ km}^2$) of temporally varying surface elevation; it is one of 11 active subglacial lakes documented beneath the WIS⁵. SLW fills and drains every few years as part of a series of hydrologically linked subglacial lakes in the area, eventually draining to the ocean^{5,28,31}. Ice-penetrating radar and active-source seismic data estimated that the maximum lake depth does not exceed 8 and 15 m at low- and high-stand, respectively^{14,32}. A lake-level rise of ~5 m from the low-stand lake level plus ice-flexural effects are sufficient to initiate flow over a drainage divide and trigger lake drainage. During a drainage event, ~0.15 km³ of water drains in a six-month timeframe at a water flux of ~10 m³ s⁻¹ (ref 5, 14). Thus, SLW is a shallow active hydrological reservoir beneath an active ice stream. The deepest point in the seismically detected water column was selected as the drill site (S 84.240° W 153.694°; Fig. 1). Drilling and subglacial lake access occurred during a near low-stand state in late January 2013³³.

Hot water drilling and clean access to SLW. A hot water drilling system was used between 23-27 January 2013 to melt through the ~801 m thick ice sheet, creating an access borehole (minimum diameter ~ 60 cm) for direct sampling and to conduct in situ measurements of the SLW water column and sediments. Microbial cells in the drilling water and on exposed surfaces of the hose, cables, and deployed equipment were reduced and killed through the use of four complementary technologies: (1) filtration, (2) UV irradiation, (3) pasteurization, and (4) disinfection with 3% w/v H₂O₂¹¹. The drilling water, derived from the overlying ice sheet, was continuously circulated through a water treatment system that removed micron and sub-micron sized particles (>0.2 µm), irradiated the drilling water with two germicidal wavelengths of UV radiation (185 nm ~40,000 µW s⁻¹ cm⁻² and 254 nm ~175,000 µW s⁻¹ cm⁻²), and pasteurized the

water at 90°C to reduce the viability of persisting microbial contamination. Ports were plumbed along the systems' flow path, allowing discrete water samples to be obtained before and after each stage¹¹. The drill hose and instrument cables were deployed at a rate no greater than 1 m s⁻¹ through a custom borehole collar that contained 12 amalgam pellet UV lamps, providing a cumulative germicidal UV dosage of at least 40,000 $\mu\text{W s}^{-1} \text{cm}^{-2}$ (Arapahoe SciTech). All borehole sampling tools and instruments were spray-saturated with 3% w/v H₂O₂ and staged in sealed polyethylene bags until tool deployment. Single-use protective apparel (Tyvek®) was worn by all personnel during borehole science operations. The efficacy of the clean access technology and procedures were tested thoroughly before use in the field and are detailed elsewhere¹¹.

Drilling was conducted at a flow rate of ~136 L min⁻¹ to ~700 mbs, whereupon the drill was withdrawn, the borehole was inspected with video, and a hydrocast was conducted at 672 mbs to measure the chemical and microbiological properties of the borehole water. To ensure that borehole water did not enter the lake upon breakthrough, the borehole hydrostatic pressure was reduced by ~35% (i.e., the water level was lowered from 80 to 108 mbs) below the expected equilibration level for 800 m of ice¹⁴. Drilling subsequently proceeded at the reduced flow rate of 19 L min⁻¹, and at 0802 on 27 January (UTC+12), the load on the hose diminished as the drill reached ~801 mbs. Two minutes later, the head above the borehole water return pump (stationed at 110 mbs) rose rapidly and remained at ~80 mbs, confirming hydrostatic equilibration between the borehole and lake water (i.e., breakthrough to SLW). Importantly, the rise in borehole water confirmed that no drilling water entered the subglacial environment during breakthrough. To maintain the borehole and offset freeze back, thermal energy was added to the borehole by redeploying the drill at a flow rate of ~135 L min⁻¹. Borehole reaming was conducted after

breakthrough to the lake by slowly withdrawing the drill ($\sim 0.01 \text{ m s}^{-1}$). A second 24 h reaming occurred 32 h after initial penetration of the lake to ensure successful deployment of all sampling tools. All in situ measurements and discrete sampling occurred over a 4 d period.

Temperature and depth. A SBE 19*plus*V2 SeaCAT Profiler CTD (Seabird Electronics,

270 Inc.) was used to measure temperature and depth within the borehole and lake water column. The instrument was deployed in profiling mode and lowered at a rate of $\sim 0.5 \text{ m s}^{-1}$. Borehole depths are referenced to the snow surface in proximity to the borehole. The water column depth in SLW (i.e., the distance between the ice-water interface and underlying sediments) was estimated using CTD data to distinguish differences in water mass upon entry to the lake water column from the
275 borehole. Lake depth was obtained from the top of the lake water mass to the depth where the sonde contacted the bottom. This depth estimate was corroborated with a calibrated cable attached to a real-time borehole video camera.

Water and sediment sampling. Following Priscu et al.¹¹, discrete samples of the drilling water ($\sim 20 \text{ L}$) were obtained at two time points during the drilling process. Samples of water
280 from the input to the filtration module, input to the borehole, water returning from the borehole, and a hydrocast at 672 mbs before lake entry were collected and concentrated onto 142 mm $0.2 \mu\text{m}$ Supor membrane filters (Pall Corporation). The filters were processed identically to those from the SLW water column (see below).

Three discrete water samples were collected between 28 and 31 January 2013 at
285 approximately mid-depth in the $\sim 2.2 \text{ m}$ SLW water column. Bulk water was collected using 10 L Niskin bottles and transferred via acid (10% HCl) leached silicon tubing to clean bottles

following the limnological procedures outlined by the McMurdo Long Term Ecological Research (LTER) Program³⁴.

SLW water column particulate matter for nucleic acid analysis was filter concentrated *in*
290 *situ* using a Large Volume Water Transfer System (WTS-LV) that was modified to fit the
minimum borehole diameter of 30 cm (McLane Research Laboratories Inc.). The WTS-LV has a
3-tier 142 mm filter holder that accepts filters in series for size fractionation of particulates in the
sample water. There were three separate casts of the WTS-LV in SLW and between 4.9 and 7.2
L of water was filter-concentrated during each 2 h deployment. In cast 1, the filter housing was
295 loaded with a 10 μm nylon mesh screen together with 3 μm and 0.2 μm Supor membrane filters.
The filters for cast 2 and 3 had pore sizes of 3.0 μm , 0.8 μm , and 0.2 μm . Immediately after
recovery, the filter housing unit was detached from the pump and opened in a class 100 laminar
flow hood. The filters were placed in sterile 142 mm petri dishes, sliced into quarters with a
clean scalpel, and transferred to a cryovial that contained 7 mL of DNA lysis solution (40mM
300 EDTA pH 8.0, 50 mM tris pH 8.3, 0.73 M sucrose). The preserved samples were immediately
frozen for transport to McMurdo Station and stored at -80°C .

Surficial sediments were collected using a multicoring device (Uwitec) that had a core
barrel inner diameter of 59.5 mm. Sediment pore water was obtained by inserting Rhizon
samplers³⁵ (0.2 μm pore size) through predrilled holes in the core barrel liner and extracted under
305 negative pressure created with a 10 mL sterile syringe. Surficial sediment (0 to 2 cm depth) from
the cores was sampled inside a class 100 clean hood using a cleaned core cutter (Uwitec). The
sediment samples for molecular biological analysis were placed in 60 mL sterile Nalgene bottles
containing 10 mL of the DNA lysis solution and frozen.

Specific electrical conductivity (EC @ 25 °C) and pH of the lake and sediment pore water were determined using a YSI model 3252 probe connected to a YSI model 3100 conductivity meter and a Beckman model 200 pH meter. Both probe and meter combinations were calibrated immediately before sample measurements were made.

Inorganic and organic chemistry. Particulate organic C (PC) and N (PN) samples from the water column were vacuum (~0.3 atm) filtered onto pre-combusted (450°C for 4 h) Whatman GF/F filters and analyzed on a CE Instruments Flash EA 112 (ThermoQuest, San Jose, CA). The filters and sediment samples which had been dewatered via centrifugation were fumed for 24 h over fresh 12 M HCl to remove inorganic carbon and dried for 24 h at 90°C before analysis. Dissolved oxygen was measured using the azide modification of the mini-Winkler titration³⁶. Dissolved inorganic carbon was measured by infrared gas analysis of acid sparged samples. Samples for dissolved inorganic N and P were filtered through pre-combusted and 1% HCl leached GF/F filters, collected in 1% HCl leached HDPE bottles, and frozen for shipment to the US where nitrate, nitrite, ammonium, and soluble reactive P were analyzed colorimetrically³⁴. Major ions and organic acids from SLW water and sediment porewater were analyzed on a Metrohm ion chromatograph using a C4 cation column and a Supp 5 anion column.

Stable isotope analysis. Stable isotope measurements were conducted at the Isolab (University of Washington, Seattle). Measurements of oxygen isotope ratios of lake water and pore water samples were made using a Picarro cavity ring-down laser spectrometer. Nitrate for $\Delta^{17}\text{O}$ determination in the water samples was concentrated using an anionic resin³⁷ followed by the bacterial reduction and thermal decomposition method^{38,39}. $\Delta^{17}\text{O}\text{-NO}_3$ was analyzed with a Finnigan Delta Plus Advantage isotope ratio mass spectrometer. Isotope measurements are

reported using standard δ notation in per mille relative to Vienna Standard Mean Ocean Water (VSMOW).

pH and oxidation-reduction measurements. Sediment pH was measured with a Microelectrodes Inc. MI-407P needle pH electrode and a MI 401 Ag/AgCl₂ micro reference electrode, calibrated with Orion low ionic strength buffers (pH 4, 7, 10). Oxidation-reduction potential (ORP) was measured in SLW water with a glass epoxy platinum electrode and a MI 401 Ag/AgCl₂ micro reference electrode calibrated with Zobell's solution and corrected to the standard hydrogen electrode (SHE).

Cell and ATP concentration. Samples for cell enumeration from water and sediment were collected in combusted glass bottles and fixed in sodium borate-buffered formalin (2% v/v). Sub-samples were filtered on black 0.2 μ m polycarbonate membrane filters, stained with SYBR Gold (Life Technologies), and immediately counted via epifluorescence microscopy. Sediment interference did not allow accurate determination of cell density in sediment samples. Cellular ATP was measured in triplicate as previously described¹¹ and viable biomass was estimated from the ATP concentration using a carbon to ATP ratio of 250 by weight^{10,21}.

Scanning electron microscopy. Samples for scanning electron microscopy (SEM) were fixed with either 2% (w/v) formalin or 0.5% (w/v) glutaraldehyde and filtered onto a 13 mm diameter 0.2 μ m polytetrafluoroethylene (PTFE) filters. Following ethanol dehydration and critical point drying, the filters were attached to an aluminum stub, coated with either gold or palladium, and observed on a Zeiss Supra 55VP Field Emission Scanning Electron Microscope.

Heterotrophic and chemoautotrophic production. Heterotrophic productivity was measured using [³H]*methyl*-thymidine incorporation into DNA⁴⁰ and [³H]leucine incorporation

into protein⁴¹. Samples [1.5 mL; 10 and 5 live and 10 and 5 trichloroacetic acid (TCA)-killed controls for casts 1 and 3, respectively] were incubated with 20 nM radiolabeled thymidine (specific activity 20 Ci mmol⁻¹) or leucine (specific activity 84 Ci mmol⁻¹) at 4°C in the dark for 175 h (average). A separate time-course experiment (data not shown) revealed that incorporation was linear over this incubation period. Incubations were terminated by the addition of 100% w/v cold TCA (5% final). Following centrifugation, a series of washes with cold 5% TCA and cold 80% v/v ethanol were performed. The final pellet was dried overnight at ~25°C. Radioactivity in the pellet was determined with a calibrated liquid scintillation counter following the addition of 1 mL of Cytoscint ES (MP Biomedicals). The rates of thymidine and leucine incorporation (nM TdR d⁻¹ or nM Leu d⁻¹) obtained at the incubation temperature (4°C) were converted to the in situ temperature of -0.49°C using an energy of activation of 48,821 J mol⁻¹ determined from temperature gradient experiments (data not shown). Rates of macromolecular synthesis were converted to carbon production using 2.0×10^{18} cells mol⁻¹ thymidine⁴² and 1.42×10^{17} cells mol⁻¹ leucine⁴³, in concert with a cellular carbon content of 11 fg C cell⁻¹ (ref 44). For the sediment assays, a slurry was created by adding 1 gram wet weight of sediment to 10 mL of 0.2 µm-filtered SLW water. The processing of the sediment slurries was identical to water samples except a total of three 80% ethanol rinses were performed to enhance the removal of unincorporated substrate. After drying, 200 µL of tissue solubilizer (ScintiGest; Fisher Chemical) was added to each vial. The metabolic rate data were normalized per gram dry weight of sediment.

Dark CO₂ fixation was determined in sterile 40 mL glass vials filled to the top with sample (leaving no headspace) and capped with PTFE lined caps (10 and 5 live and 10 and 5 TCA-killed for casts 1 and 3, respectively). The vials were amended with sterile ¹⁴C-labeled

bicarbonate (stock concentration = $0.1144 \text{ mCi mL}^{-1}$) to a final experimental concentration of 0.01 mCi mL^{-1} and incubated in the dark at 4°C for 281 h (average). A separate time-course experiment (data not shown) revealed that incorporation was linear over this incubation period. Incubations were terminated by the addition of cold TCA (2.5% w/v final concentration) and
380 filtering onto $0.2 \mu\text{m}$ polycarbonate filters. The filters were placed in 20 mL scintillation vials, acidified with 0.5 mL of 3N HCl, and dried at 60°C for 24 h. Radioactivity on the filters was determined with a calibrated liquid scintillation counter following the addition of 10 mL of Cytoscint ES (MP Biomedicals).

Molecular and phylogenetic analysis of SSU rRNA gene sequences. DNA was
385 extracted from a portion of each filter (1/8 of a 142 mm filter) using the Power Water DNA Isolation Kit and from sediments ($\sim 0.5 \text{ g}$ wet weight) with the Power Soil DNA isolation kit (MO BIO Laboratories, Inc.). The extraction procedures followed those recommended by the manufacture.

The SSU rRNA gene was amplified using the oligonucleotide primers 515F and 806R, as
390 described previously⁴⁵. Amplification reactions ($50 \mu\text{L}$ each) were performed using 5 units of AmpliTaq Gold DNA polymerase LD (Invitrogen), 1 x PCR Gold Buffer (Invitrogen), 3.5 mM MgCl_2 , 10 pmol of each primer, $200 \mu\text{M}$ dNTPs, and 0.1 - 3 ng of DNA template. The optimum number of cycles for PCR was determined by successively lowering the cycle number so that false positive amplification was prevented while amplification was possible for the lowest
395 biomass samples analyzed. After 9 min. of heat activation at 94°C (i.e., AmpliTaq Gold DNA polymerase is a chemical hot-start enzyme), 35 cycles of PCR were performed using the following amplification conditions: denaturation at 94°C for 45 s, annealing for 90 s at 50°C , and elongation at 72°C for 90 s, with a terminal elongation at 72°C for 10 min. The concentration

of the PCR products were determined using the Quant-iT PicoGreen dsDNA Assay Kit

400 (Invitrogen). The amplicons were pooled and cleaned with the MoBio UltraClean PCR Clean-Up Kit. Sequencing was performed using the Illumina MiSeq platform (Selah Genomics, Greenville, SC).

Paired end sequence reads were assembled and quality filtered using the Mothur⁴⁶ phylogenetic analysis pipeline (v1.33.2). The sequences were aligned with the SILVA

405 Incremental Aligner⁴⁷ (SINA v1.2.11; database release 115). The aligned reads were checked for chimeras using the Uchime algorithm⁴⁸, as implemented within Mothur, and chimeric sequences were removed from the data. Sequences with >97% SSU rRNA gene sequence similarity were clustered into an OTU and representative sequences for each OTU were chosen for classification using the SILVA database. Diversity and richness estimates were calculated in Mothur⁴⁶.

410 Singletons were excluded from further analyses, and for simplicity of presentation, phyla represented by <1% of the sequence reads were grouped into the unclassified category (Fig. 3a).

Community comparisons using Yue and Clayton theta similarity coefficient analysis and

Weighted Unifrac were also performed within Mothur. MEGA 5.2 software was used for

phylogenetic analysis using maximum likelihood, the Jukes-Cantor nucleotide substitution model

415 (1000 iterations), and a 253 nucleotide alignment. The SSU sequence data were deposited in the NCBI SRA database under the accession number SRP041285. Attempts to detect SSU sequences from eukaryotes were based on previously published methods⁵⁰.

Methods References

31. Carter, S. P. & Fricker, H. A. The supply of subglacial meltwater to the grounding line of the Siple Coast, West Antarctica. *Ann. Glaciol.* 53, 267-290 (2012)
32. Horgan, H. J., *et al.* Subglacial Lake Whillans—Seismic observations of a shallow active reservoir beneath a West Antarctic ice stream. *Earth Planet. Sci. Lett.* 331-332, 201-209 (2012)
33. Siegfried, M. R., Fricker, H. A., Roberts, M., Scambos, T. A. & Tulaczyk, S. A decade of West Antarctic subglacial lake interactions from combined ICESat and CryoSat-2 altimetry. *Geophys. Res. Lett.* 2013GL058616, doi:10.1002/2013GL058616 (2014)
34. Priscu, J. C. LTER Limno Methods Manual – MCM_Limno_Methods_current.pdf. http://www.mcmlter.org/data/lakes/MCM_Limno_Methods_current.pdf (2013)
35. Seeberg-Elverfeldt, J., Schlüter, M., Feseker, T. & Kölling, M. Rhizon sampling of porewaters near the sediment-water interface of aquatic systems. *Limnol. Oceanogr. Methods* 3, 361–371 (2005)
36. American Public Health Association. *Standard methods for the examination of water and waste water* (American Public Health Society Press, 1995)
37. Costa, A. W. *et al.* Analysis of atmospheric inputs of nitrate to a temperate forest ecosystem from $\Delta^{17}\text{O}$ isotope ratio measurements. *Geophys. Res. Lett.* 38, L15805, (2011).
38. Casciotti, K. L., Sigman, D. M., Galanter Hastings, M., Bohlke, J. K. & Hilkert, A. Measurement of the oxygen isotopic composition of nitrate in seawater and freshwater using the denitrifier method. *Anal. Chem.* 74, 4905-4912 (2002).

39. Kaiser, J., Hastings, M. G., Houlton, B. Z., Rockmann, T. & Sigman, D. M. Triple oxygen isotope analysis of nitrate using the denitrifier method and thermal decomposition of N₂O. *Anal. Chem.* 79, 599–607 (2007)
40. Fuhrman, J. & Azam, F. Thymidine incorporation as a measure of heterotrophic bacterioplankton production in marine surface waters: evaluation and field results. *Mar. Biol.* 66, 109-120 (1982)
41. Kirchman, D., K'nees, E. & Hodson, R. Leucine incorporation and its potential as a measure of protein synthesis by bacteria in natural aquatic systems. *Appl. Environ. Microbiol.* 49, 599-607 (1985)
42. Bell, R. T. Estimating production of heterotrophic bacterioplankton via incorporation of tritiated thymidine. In: Kemp, P. F., Sherr, B. F., Sherr, E. B. & Cole, J. J. (eds) *Handbook of Methods in Aquatic Ecology* (Lewis, 1993)
43. Chin-Leo, G. & Kirchman, D. Estimating bacterial production in marine waters from the simultaneous incorporation of thymidine and leucine. *Appl. Environ. Microbiol.* 54, 1934-1939 (1988)
44. Kepner, R. L., Wharton Jr., R. & Suttle, C.A. Viruses in Antarctic Lakes. *Limnol. Oceanogr.* 43, 1754-1761 (1998)
45. Caporaso, J. G. *et al.* Ultra-high-throughput microbial community analysis on the Illumina HiSeq and MiSeq platforms. *ISME J.* 6, 1621-1624 (2012)
46. Schloss, P.D. *et al.* Introducing mothur: open-source, platform-independent, community-supported software for describing and comparing microbial communities. *Appl. Environ. Microbiol.* 75, 7537-7541 (2009)

47. Pruesse, E., Peplies, J. & Glöckner, F.O. SINA: accurate high-throughput multiple sequence alignment of ribosomal RNA genes. *Bioinformatics* 28, 1823-1829 (2012)
48. Edgar, R. C., Haas, B. J., Clemente, J.C., Quince, C. & Knight, R. UCHIME improves sensitivity and speed of chimera detection. *Bioinformatics* 27, 2194-2200 (2011)
49. Holland, H. D. *The Chemistry of the Atmosphere and Oceans* (Wiley, 1978)
50. Amaral-Zettler, L. A., McCliment, E. A., Ducklow, H. W. & Huse, S. M. A method for studying protistan diversity using massively parallel sequencing of V9 hypervariable regions of small-subunit ribosomal RNA genes. *PLoS ONE* 4, e6372 (2009)

Accepted 9 July 2014

Extended data table legends

Extended Data Table 1 Crustal and seawater components to SLW waters

Extended Data Table 2 Summary of parameters for the SLW SSU gene sequence data

Accepted 9 July 2014

Supplementary Information

1. Extended Data Table 1. This table contains information on the crustal and seawater components to SLW waters.
2. Extended Data Table 2. This table contains information on the SLW SSU gene sequence data.
3. Supplemental Information. This file contains the Supplemental Discussion and additional references.

Acknowledgements

The Whillans Ice Stream Subglacial Access Research Drilling (WISSARD) project was funded by National Science Foundation grants (0838933, 0838896, 0838941, 0839142, 0839059, 0838885, 0838855, 0838763, 0839107, 0838947, 0838854, 0838764 and 1142123) from the Division of Polar Programs. Partial support was also provided by funds from NSF award 1023233 (B.C.C.), NSF award 1115245 (J.C.P), the NSF's Graduate Research Fellowship Program (1247192; A.M.A.), the Italian National Antarctic Program (C.B.), and fellowships from the NSF's IGERT Program (0654336) and the Montana Space Grant Consortium (A.B.M.). Logistics were provided by the 139th Expeditionary Airlift Squadron of the New York Air National Guard, Kenn Borek Air, and by many dedicated individuals working as part of the Antarctic Support Contractor, managed by Lockheed-Martin. The drilling was directed by F. Rack (University of Nebraska - Lincoln); D. Blythe, J. Burnett, C. Carpenter, D. Duling (chief driller), D. Gibson, J. Lemery, A. Melby, and G. Roberts provided drill support at SLW. L. Geng, B. Vandenheuvell, A. Schauer and E. Steig (IsoLab, University of Washington, Seattle) provided assistance with the stable isotopic analyses. We thank J. Dore for assistance with the nutrient analysis.

Author informationAffiliations

Department of Biological Sciences, Louisiana State University, Baton Rouge, Louisiana, USA

Brent C. Christner & Amanda M. Achberger

Department of Land Resources and Environmental Science, Montana State University, Bozeman, Montana, USA

John C. Priscu, Alexander B. Michaud & Trista J. Vick-Majors

Institute for the Dynamics of Environmental Processes – CNR, Venice, and Department of Environmental Sciences, University of Venice, Venice, Italy

Carlo Barbante

Institute of Geophysics and Planetary Physics, Scripps Institution of Oceanography, University of California San Diego, La Jolla, CA, USA

Sasha P. Carter

Physics Department, St. Olaf College, Northfield, MN, USA

Knut Christianson

Department of Microbiology, University of Tennessee, Knoxville, TN, USA

Jill A. Mikucki

Department of Geography and Earth Sciences, Aberystwyth University, Aberystwyth, UK

Andrew C. Mitchell

Department of Earth Science, Montana State University, Bozeman, Montana, USA

Mark L. Skidmore

Present address: Courant Institute of Mathematical Sciences, New York University, New York, NY, USA

Knut Christianson

Consortia

WISSARD Science Team Members

W.P. Adkins, S. Anandakrishnan, G. Barcheck, L. Beem, A. Behar, M. Beitch, R. Bolsey, C. Branecky, R. Edwards, A. Fisher, H. Fricker, N. Foley, B. Guthrie, T. Hodson, R. Jacobel, S. Kelley, K. Mankoff, E. McBryan, R. Powell, A. Purcell, D. Sampson, J. Severinghaus, R. Scherer, J. Sherve, M. Siegfried, and S. Tulaczyk.

Contributions

The manuscript was written by B.C.C. and J.C.P. A.M.A. generated and analyzed the molecular data; C.B., A.C.M., and M.L.S. conducted and interpreted the chemical measurements; S.P.C. and K.C. provided geophysical data; J.A.M. obtained and examined the CTD data; A.B.M. and T.J.V. contributed and analyzed physiological and biogeochemical data; M.L.S. conducted and interpreted the isotopic analyses; and T.J.V. provided the micrographs. All authors contributed to the study design and acquisition of samples and/or data.

Competing financial interests

The authors declare no competing financial interests.

Corresponding author

Correspondence to: Brent C. Christner (xner@lsu.edu) or John C. Priscu (jpriscu@montana.edu)

Accepted 9 July 2014

Table 1 Biogeochemical data from the SLW borehole, water column, and surficial sediments

| Parameter | Borehole ^a | Water Column ^b | Sediments ^c |
|--|----------------------------|--|------------------------|
| <i>Physical</i> | | | |
| Temperature (°C) ^d | -0.17 (0.25) | -0.49 (0.03) | n.d. |
| Conductivity (μS cm ⁻¹ @ 25°C) ^e | 5.3 | 720 (10) | 860 |
| pH ^e | 5.4 | 8.1 (0.1) | 7.3 |
| Redox [mV (SHE)] ^e | n.d. | 382 | n.d. |
| <i>Microbiological</i> | | | |
| Cell density (cell mL ⁻¹) | 6.9x10 ² (51.0) | 1.3x10 ⁵ (0.4x10 ⁵) | n.d. |
| Cellular ATP (pmol L ⁻¹) | 0.04 (0.002) | 3.70 (1.00) | n.d. |
| ³ H-thymidine ^f | n.d. | 13.7 (1.3) | 46.6 (5.6) |
| ³ H-leucine ^f | n.d. | 2.9 (0.4) | 0.9 (0.04) |
| ¹⁴ C-bicarbonate | n.d. | 32.9 (4.2) | n.d. |
| <i>Carbon and nutrients</i> | | | |
| Dissolved Oxygen (μmol L ⁻¹) | n.d. | 71.9 (12.5) | n.d. |
| DIC (mmol L ⁻¹) | n.d. | 2.11 (0.03) | n.d. |
| DOC (μmol L ⁻¹) | n.d. | 221 (55) | n.d. |
| Acetate (μmol L ⁻¹) | n.d. | 1.3 (0.2) | n.d. |
| Formate (μmol L ⁻¹) | n.d. | 1.2 (0.3) | n.d. |
| PC ^g | n.d. | 78.5 (7.4) | 384.2 (37.0) |
| PN ^g | n.d. | 1.2 (0.4) | 21.5 (1.7) |
| PC:PN (molar) | n.d. | 65.4 (0.3) | 17.9 (0.4) |
| NH ₄ ⁺ (μmol L ⁻¹) | n.d. | 2.4 (0.6) | n.d. |
| NO ₂ ⁻ (μmol L ⁻¹) | n.d. | 0.1 (0.1) | n.d. |
| NO ₃ ⁻ (μmol L ⁻¹) | n.d. | 0.8 (0.5) | 9.1 |
| PO ₄ ³⁻ (μmol L ⁻¹) | n.d. | 3.1 (0.7) | 7.3 |
| DIN:SRP (molar) | n.d. | 1.1 (0.4) | n.d. |
| <i>Major ions (μeq L⁻¹)</i> | | | |
| Na ⁺ | n.d. | 5276 (18) | 6977 |
| K ⁺ | n.d. | 186 (4.2) | 293 (1.0) ^h |
| Mg ²⁺ | n.d. | 507 (12) | 596 (101) ^h |
| Ca ²⁺ | n.d. | 859 (29) | 860 (104) ^h |
| F ⁻ | n.d. | 31.5 (0.4) | 34.0 |
| Cl ⁻ | n.d. | 3537 (3.4) | 4943 |
| Br ⁻ | n.d. | 6 (0.01) | 7 (0.4) ^h |
| SO ₄ ²⁻ | n.d. | 1111 (0.4) | 1230 |
| HCO ₃ ⁻ | n.d. | 2111 (35) | 2238 ⁱ |
| <i>Stable isotopes ^j</i> | | | |
| δ ¹⁸ O-H ₂ O | n.d. | -38.0 ‰ | -37.5 ‰ |
| Δ ¹⁷ O-NO ₃ ⁻ | n.d. | -0.1 to 0.2 ‰ | n.d. |

^a Borehole water sampled by hydrocast at 672 mbs before lake entry.

^b Water column data represent averages (\pm SD) from hydrocasts collected on 28 January 2013 (cast 1), 30 January (casts 2), and 31 January (cast 3) 2013, except for ^3H -leucine incorporation, which is an average of cast 1 and 3 only.

^c The sediment data correspond to measurements from the upper 2 cm of surficial sediments.

^d Average (\pm SD) of in situ measurements made through the lake water column at ~ 10 cm intervals with a SBE 19*plus*V2 SeaCAT Profiler CTD on 28 January and 30 January 2013.

^e Based on measurements from discrete water samples brought to the surface.

^f Macromolecular incorporation rates of tritium were converted to cellular carbon and presented along with bicarbonate incorporation as average $\text{ng C L}^{-1} \text{ d}^{-1}$ (\pm SD) for water or average $\text{ng C d}^{-1} \text{ gram dry weight}^{-1}$ (\pm SD) of sediment.

^g Average (\pm SD) $\mu\text{mol L}^{-1}$ for water and average (\pm SD) $\mu\text{mol g dry weight sed}^{-1}$ for surficial sediment.

^h Surficial sediment porewater major ions are the average (\pm range) of two replicates.

ⁱ Calculated based on charge balance.

^j Values are per mille and reported relative to V-SMOW. The range of 2 measurements is given for $\Delta^{17}\text{O-NO}_3^-$.

n.d. = no data available.

Figure legends

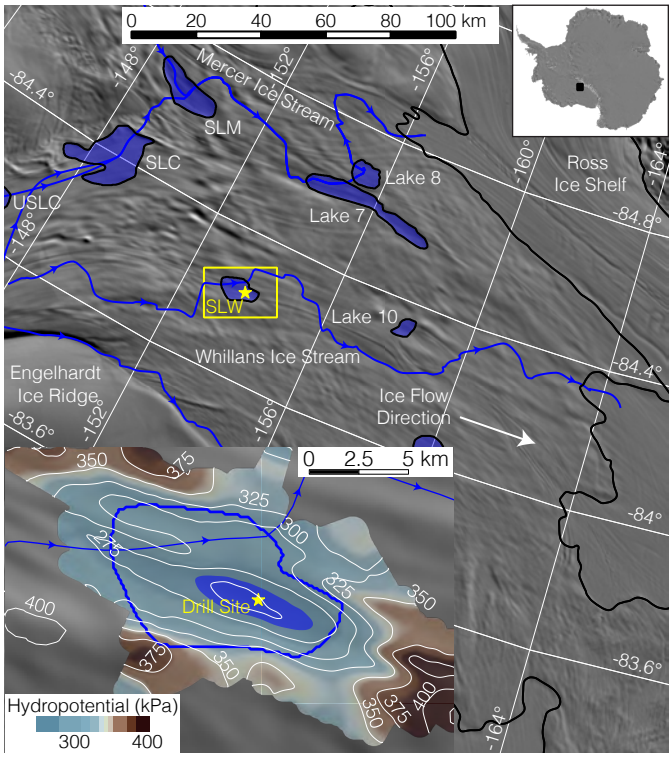
Figure 1 Locator map of the WIS and SLW. (a) The yellow box and star indicates the general location of the lake and the drill site; maximum extent of SLW and other lakes²⁸ under the ice stream are shaded in blue; predicted subglacial water flowpaths through SLW and other subglacial lakes are represented by blue lines with arrows; the black line denotes the ice-sheet grounding line at the edge of the Ross Ice Shelf²⁹. Inset (expanded from area in yellow box) shows details of SLW with both maximum (solid blue line) and minimum lake extent (shaded blue area), hydropotential contours (white isolines; 25 kPa interval), and drill site (yellow star; S 84.240° W 153.694°). Background imagery is MODIS MOA³⁰.

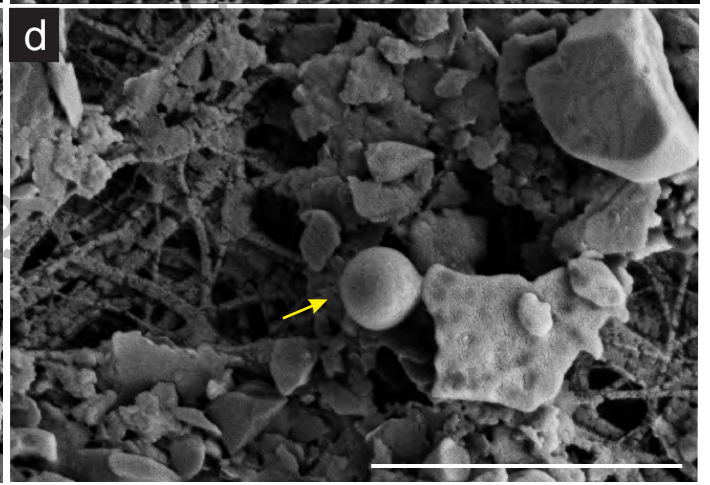
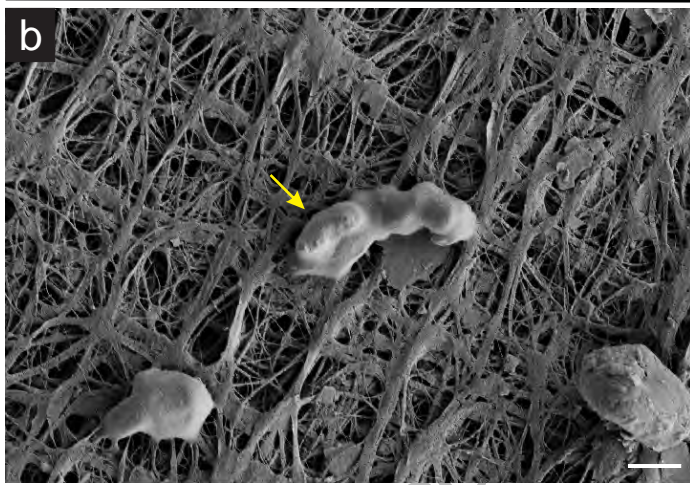
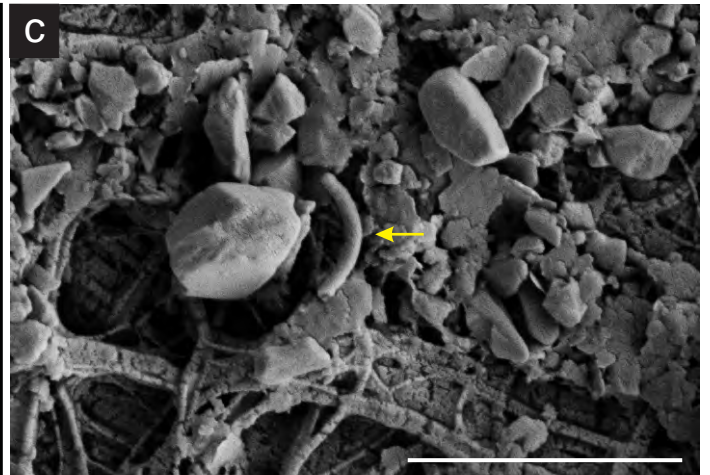
Figure 2 Morphological diversity of microbial cells in the SLW water column. (a) Epifluorescence micrograph showing a variety of cell morphotypes, which was confirmed by SEM (b-d). The yellow arrows in the SEM images indicate cells with (b) rod, (c) curved rod, and (d) coccoid morphologies. Scale bar = 2 μ m.

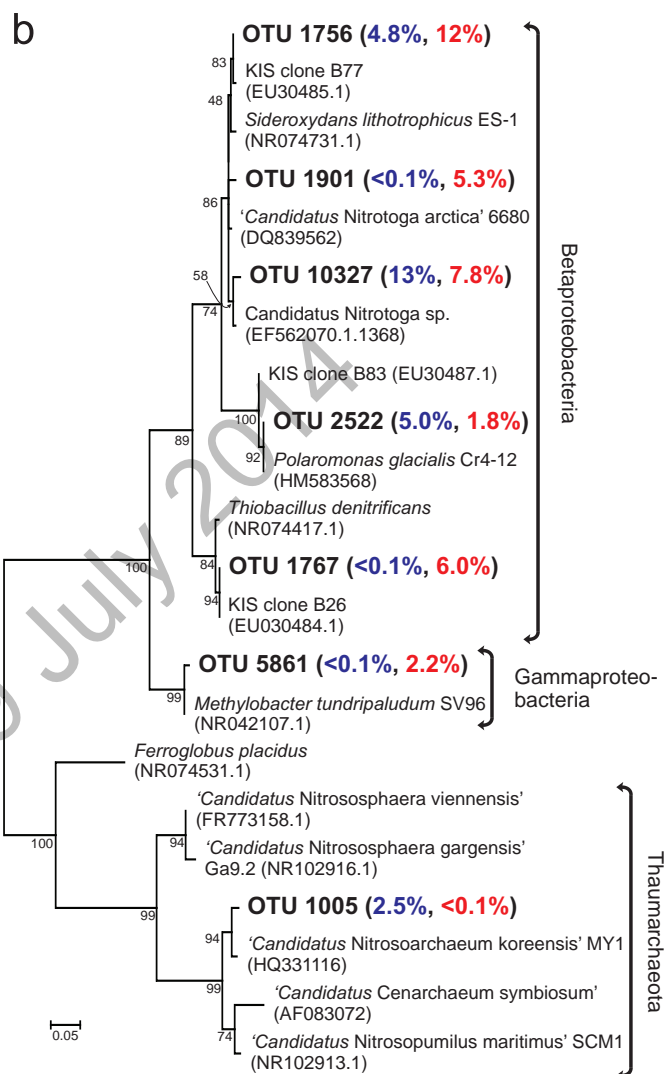
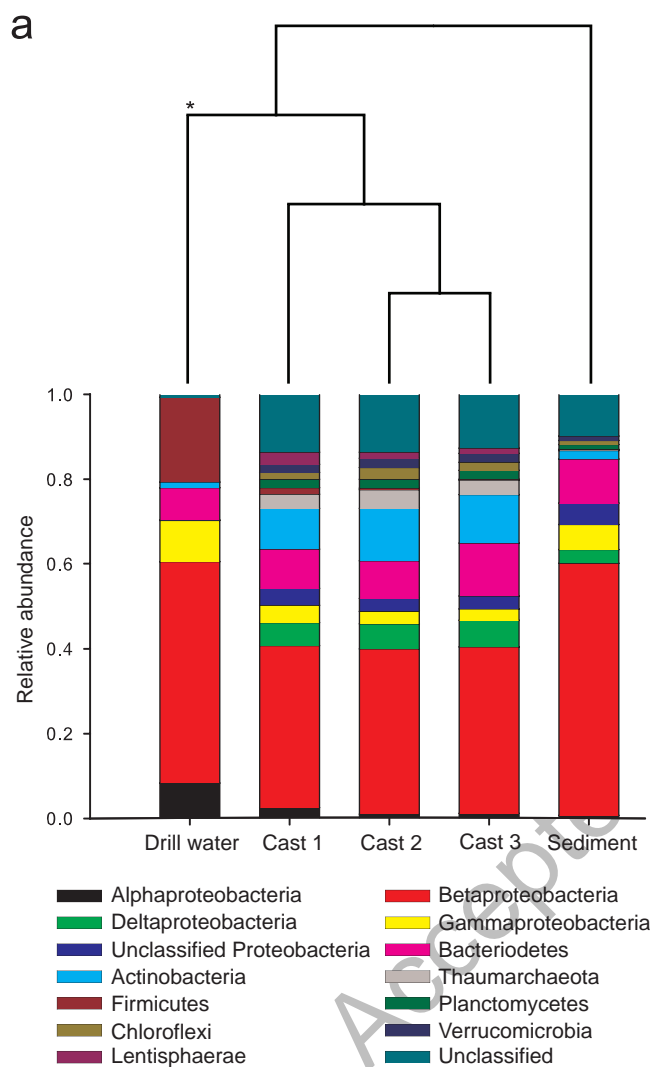
Figure 3 Phylogenetic analysis of SSU gene sequences obtained from the SLW water column, surficial sediment (0-2 cm), and drilling water. (a) Cluster analysis of the microbial phylogenetic structure in the samples (top) and the relative abundance of bacterial and archaeal phyla in the water and sediment samples (bottom). The Proteobacteria were split into classes for greater detail. The asterisk indicates statistical significance (AMOVA, p-value <0.001). (b) Phylogenetic analysis of bacterial and archaeal OTUs abundant in the SLW water column and sediments. The accession numbers of nearest neighbors and reference taxa are listed parenthetically. Bootstrap values are shown at the nodes. SLW phylotypes are bolded and followed by the percentage each

represented in the water column (blue) and sediment (red) libraries. The scale bar indicates the number of nucleotide substitutions per position.

Accepted 9 July 2014







Extended Data Table 1 | Crustal and seawater components to SLW waters

| Sample | $\mu\text{eq L}^{-1}$ | | | | | | | |
|--|-----------------------|--------------|------------------|------------------|--------------|---------------|--------------------|------------------|
| | Na^+ | K^+ | Mg^{2+} | Ca^{2+} | F^- | Cl^- | SO_4^{2-} | HCO_3^- |
| SLW Average * | 5276 | 186 | 507 | 859 | 31.5 | 3537 | 1111 | 2111 |
| Sea water component † | 3038 | 66 | 691 | 132 | 0.4 | 3537 | 366 | 16 |
| Non-seawater, crustal weathering component ‡ | 2239 | 120 | -183 § | 726 | 31.1 | 0 | 745 | 2096 |

* Average values for hydrocasts 1, 2 and 3.

† Calculated using Cl^- concentrations and ratios of each species to Cl^- in seawater in $\mu\text{eq L}^{-1}$; Na^+ 0.859, K^+ 0.019, Mg^{2+} 0.195, Ca^{2+} 0.037, F^- 0.00013, SO_4^{2-} 0.103, and HCO_3^- 0.004⁴⁹.

‡ Calculated by subtracting the seawater component from the average SLW solute concentration for each ion.

§ Negative values indicate the potential for ion exchange of Mg^{2+} with other cations on clay minerals present in suspended sediments of SLW.

Extended Data Table 2 | Summary of parameters for the SLW SSU gene sequence data

| Site | Number of Sequences * | Number of OTUs † | Coverage ‡ | Inverse Simpson Diversity Index ‡ | Shannon Diversity Index ‡ | Chao Richness Estimator ‡ |
|--------------------------|-----------------------|------------------|------------|-----------------------------------|---------------------------|---------------------------|
| Drill and borehole water | 984,412 | 962 | 99.8% | 11.0 | 3.4 | 5,370 |
| SLW water column | 2,686,526 | 3,931 | 99.5% | 35.3 | 4.9 | 41,603 |
| SLW sediments | 333,600 | 2,424 | 97.3% | 31.8 | 5.1 | 42,079 |

* Sequences remaining after quality filtering, and removal of chimeric sequences and singletons.

† OTUs that passed quality filtering, excluding singletons.

‡ Calculated using Mothur⁴⁶.

Supplementary Discussion

Solute sources for SLW waters. The Cl^- to Br^- ratios of SLW waters averaged 0.00164, which is close to that for seawater (0.00156)⁴⁹. Thus a parsimonious assumption is that all Cl^- and Br^- in SLW was from a seawater source. The average Cl^- concentration of 3.5 mmol L⁻¹ in SLW represents a dilution relative to seawater of ~154-fold, indicating that seawater was a volumetrically minor contribution to the lake water. The seawater component for other major anions and cations can then be calculated using Cl^- concentrations and ratios of each species to Cl^- in seawater in $\mu\text{eq L}^{-1}$ (Extended Data Table 1). The crustally-derived component of solute to SLW was determined by subtracting the seawater values for individual ions from the average SLW composition (Extended Data Table 1). This calculation results in negative values for Mg^{2+} , indicating a deficit of Mg^{2+} relative to seawater ratios. A process that could account for the Mg^{2+} deficit is an ion exchange reaction with other cations on clay minerals present in suspended sediments of SLW. Theoretical and observational data indicate that seawater may penetrate no further than a few kilometers inland of the low-tide grounding line, making a seawater incursion to SLW (~100 km from the grounding line) extremely unlikely. Therefore, we hypothesize that the seawater source is from pre-existing marine pore waters in sediments beneath and upstream of SLW.

The inorganic nitrogen pool within the water column of SLW was dominated by ammonium relative to nitrite and nitrate (Table 1). Since mineral sources of ammonium are minor, the majority of the ammonium is presumed to originate from the microbial mineralization of nitrogen-containing organic material in the sediments, which could diffuse into the water column and also be transported to SLW from upstream portions of the subglacial hydrological

network. A 1:1 relationship would be expected between NH_4^+ loss and NO_3^- gain unless N_2O or other intermediates were being produced by nitrification. Given the low oxygen concentrations, high NH_4^+ , and SSU sequence data suggesting that nitrifying taxa were abundant in the SLW water column (Fig. 3b), the production of N_2O is likely⁵¹. Unfortunately, we do not have N_2O concentration data for SLW water. The unexpectedly low nitrate level may also result from denitrification in the sediment surface layers or in low oxygen microzones associated with suspended sediment particles. Our sequence data revealed the presence of known denitrifiers (*Thiobacillus denitrificans*) and nitrate reducers (e.g., species of *Polaromonas*), supporting this contention.

Molecular analysis of SSU gene sequences. Paired-end sequencing of the V4 region of the SSU gene generated 3,556,417 sequences from the SLW water column, 1,361,815 from the drill and borehole water, and 561,966 from the surficial sediment samples. After quality filtering and removal of chimeric sequences, 2,686,526, 984,412, and 333,600, respectively, reads were used for phylogenetic analysis (Extended Data Table 2). Calculation of sequence coverage (Extended Data Table 2) and collector curves (data not shown) indicated the depth of sequencing to be sufficient to describe the abundant members in the SLW water and sediment communities.

Analysis of molecular variance (AMOVA) in data obtained from three casts of the WTS-LV showed no statistical difference amongst the casts (pair wise p-values ≥ 0.69); therefore, all molecular data from the water column were compiled. Estimations of species diversity in the lake water revealed a community diversity comparable to many surface aquatic environments⁵⁰. Of the 3,931 OTUs identified in the SLW water column, 3,105 (87% of the total sequence reads) and 30 (3.6% of the total sequence reads) classified within the *Bacteria* and *Archaea*, respectively, while 793 OTUs were not classified. The bacterial and archaeal OTUs were

classified into 32 and 2 phyla, respectively (Fig. 3A). The majority of OTUs were taxonomically affiliated with the Proteobacteria (1,893 OTUs; 53% of all sequences) and Actinobacteria (401 OTUs; 11% of all sequences).

50 Within the proteobacterial OTUs from the water column, 84% of the sequences classified within the beta- and delta- classes. Phylotypes most closely related to species in the genera ‘*Candidatus Nitrotoga*’, *Polaromonas*, and *Sideroxydans* were the 1st, 2nd, and 3rd, respectively, most abundant OTUs in the dataset. Highly abundant actinobacterial phylotypes were most closely related to SSU gene sequences reported previously from polar lake environments (e.g.,
55 ref 52). Most of the archaeal phylotypes were classified as Thaumarchaeota, with one OTU from this group representing the 5th most abundant phylotype. Phylotypes that were abundant in the water column and surficial sediment (Fig. 3b) were very rare (OTU 1756, 0.003%; OTU 10327, 0.007%; OTU 2522, 0.002%; and OTU 1767, 0.001%) or not observed (OTU 1901, OTU 5861, and OTU 1005) in data obtained from the drill water assemblage.

60 Nearly all the SSU gene sequences characterized from the surficial sediment were bacterial (1,935 OTUs; 94%), with only 0.3% classifying within the *Archaea*. Proteobacteria were the most abundant phylum, with the beta- and gamma- classes representing 65% of the OTUs within this group. Similar to observations for the SLW water column, phylotypes most closely related to species of *Sideroxydans* and ‘*Candidatus Nitrotoga*’ were the most abundant
65 OTUs (1st and 2nd, respectively). However, phylotypes that classified within the genera *Thiobacillus*, *Nitrosospira*, and *Methylobacter* were enriched in the sediments relative to the water column (<0.7% of all sequences in the water column). Cluster analysis of the water column, sediment, and drilling water community structure indicated that the SLW water and

surficial sediments were not statistically different; however, the drilling water was statistically
70 different from the water column and sediment environment (Figure 3a).

Samples of the drilling water contained no OTUs that classified as archaeal, and only 41
OTUs (<1%) were unclassifiable at the domain level. The Proteobacteria and the Firmicutes
were the most abundant phyla in the dataset, representing 70% and 20% of the sequences,
respectively. The most abundant phylotypes were most closely related to species of
75 *Janthinobacterium* and *Tumebacillus*, with each representing ~19% of the dataset. Many of the
other abundant OTUs in the drilling water were closely related to sequences and isolates
observed previously in icy environments, including Antarctic ice cores⁵³.

Accepted 9 July 2014

Supplementary Discussion References

50. Biers, E. J., Sun, S. & Howard, E. C. Prokaryotic genomes and diversity in surface ocean waters: interrogating the global ocean sampling metagenome. *Appl. Environ. Microbiol.* 75, 2221-2229 (2009)
51. Goreau, R. E. *et al.* Production of NO_2^- and N_2O by nitrifying bacteria at reduced concentrations of oxygen. *Appl. Environ. Microbiol.* 40, 526–532 (1980).
52. Mosier, A. C., Murray, A. E. & Fritsen, C. H. Microbiota within the perennial ice cover of Lake Vida, Antarctica. *FEMS Microbiol. Ecol.* 59, 274-288 (2007)
53. Raymond, J. A., Christner, B.C. & Schuster, S. C. A bacterial ice-binding protein from the Vostok Ice Core. *Extremophiles* 12, 713-717 (2008)